



Research Article

Highly Dispersive Optical Solitons with Differential Group Delay for Kerr Law of Self-Phase Modulation by Sardar Sub-Equation Approach

Anwar Ja'afar Mohamad Jawad¹, Yakup Yildirim^{2,3,4*}, Anjan Biswas^{5,6,7,8,9} , Ibraheem Kasim Ibraheem^{10,11}, Ali Saleh Alshomrani⁶

¹Department of Computer Technical Engineering, Al-Rafidain University College, Baghdad-10064, Iraq

²Department of Computer Engineering, Biruni University, Istanbul-34010, Turkey

³Mathematics Research Center, Near East University, 99138 Nicosia, Cyprus

⁴Faculty of Arts and Sciences, University of Kyrenia, 99320 Kyrenia, Cyprus

⁵Department of Mathematics and Physics, Grambling State University, Grambling, LA 71245-2715, USA

⁶Mathematical Modeling and Applied Computation Research Group, Center of Modern Mathematical Sciences and their Applications Department of Mathematics, King Abdulaziz University, Jeddah-21589, Saudi Arabia

⁷Department of Applied Sciences, Cross-Border Faculty of Humanities, Economics and Engineering, Dunare de Jos University of Galati, 111 Domneasca Street, Galati-800201, Romania

⁸Department of Mathematics and Applied Mathematics, Sefako Makgatho Health Sciences University, Medunsa-0204, Pretoria, South Africa

⁹Department of Applied Mathematics, National Research Nuclear University, Moscow-115409, Russian Federation

¹⁰Department of Electrical Engineering, College of Engineering, University of Baghdad, Baghdad-10001, Iraq

¹¹Department of Electronics and Communication Engineering, Uruk University, Baghdad, Iraq
E-mail: yakupyildirim110@gmail.com

Received: 25 June 2024; **Revised:** 14 August 2024; **Accepted:** 9 September 2024

Abstract: The paper reports highly dispersive optical soliton solutions that are recovered with differential group delay with Kerr law of self-phase modulation. The Sardar's sub-equation approach is implemented for this retrieval. A full spectrum of optical solitons has been thus recovered. The parameter constraints are also displayed for the existence of such solitons.

Keywords: concatenation, solitons, dispersion, constraints, Sardar's sub-equation

MSC: 78A60

1. Introduction

The concept of highly dispersive optical solitons was conceived slightly less than a decade ago when the chromatic dispersion ran low [1-5]. The low count of dispersion is replenished with higher order ones that would lead to the concept of highly dispersive optical solitons [6-10]. These additional dispersive effects stem from inter-modal dispersion (IMD), third-order dispersion (3OD), fourth-order dispersion (4OD), fifth-order dispersion (5OD) and finally the sixth-order dispersion (6OD). One of the cons with this concept of highly dispersive optical solitons, as the title implies, is

that the solitons would be rendered to be dispersive and thus significant soliton radiation would ensue. Additionally, the solitons would also be drastically slow. From a mathematical standpoint, these effects are ignored and the integrability of the model is being focused on.

The model has been studied extensively for the scalar version [11-15]. The soliton solutions have been revealed and the conservation laws have been recovered [16-20]. The current paper turns the page. The model is studied with Kerr law of self-phase modulation (SPM) with differential group delay. The governing model is first written with polarization-mode dispersion and subsequently the Sardar sub-equation approach has been implemented to recover its soliton solutions. A full spectrum of soliton solutions has been thus recovered. The parameter constraints for the existence of such solitons that naturally emerge from the analysis are also presented. The numerical simulations also support the analysis.

2. Governing Model

The scalar form of the nonlinear Schrödinger equation (NLSE), which models the propagation of solitons through an optical fiber, is expressed as [1-5]:

$$iq_t + ia_1q_x + a_2q_{xx} + ia_3q_{xxx} + a_4q_{xxxx} + ia_5q_{xxxxx} + a_6q_{xxxxxx} + F(|q|^2)q = 0, \quad (1)$$

where $q(x, t)$ is a complex-valued function representing the wave profile. The independent variables x and t denote the spatial and temporal coordinates, respectively, and $i = \sqrt{-1}$. The real-valued coefficients a_j for $1 \leq j \leq 6$ represent intermodal dispersion (IMD), chromatic dispersion (CD), third-order dispersion (3OD), fourth-order dispersion (4OD), fifth-order dispersion (5OD), and sixth-order dispersion (6OD), respectively. Lastly, the functional F describes the nonlinear self-phase modulation (SPM) as:

$$F(|q|^2)q \in U_{m,n=1}^{\infty} C^k((-n, n) \times (-m, m); R^2).$$

The NLSE for highly dispersive optical solitons with the Kerr law of refractive index in a polarization-preserving optical fiber is expressed as:

$$iq_t + ia_1q_x + a_2q_{xx} + ia_3q_{xxx} + a_4q_{xxxx} + ia_5q_{xxxxx} + a_6q_{xxxxxx} + c|q|^2q = 0, \quad (2)$$

where the constant c is the coefficient of the Kerr law nonlinearity. For birefringent fibers, this model separates into two components as follows:

$$\begin{aligned} &iu_t + ia_1u_x + a_2u_{xx} + ia_3u_{xxx} + a_4u_{xxxx} + ia_5u_{xxxxx} \\ &+ a_6u_{xxxxxx} + (c_1|u|^2 + c_2|v|^2)u = 0, \end{aligned} \quad (3)$$

and

$$\begin{aligned} &iv_t + ib_1v_x + b_2v_{xx} + ib_3v_{xxx} + b_4v_{xxxx} + ib_5v_{xxxxx} + b_6v_{xxxxxx} \\ &+ (d_1|v|^2 + d_2|u|^2)v = 0. \end{aligned} \quad (4)$$

3. Travelling wave solution

To address the coupled system (3), we assume the following solution structure:

$$u(x, t) = U_1(\xi)e^{i\phi(x,t)}, \quad (5)$$

$$v(x, t) = U_2(\xi)e^{i\phi(x,t)}, \quad (6)$$

where $\xi = x - \gamma t$ and the real-valued phase component is $\phi(x, t) = -kx + \omega t + \phi_0$, while $U_1(\xi)$ and $U_2(\xi)$ are the real-valued amplitude components of the wave. Here, γ is the soliton velocity, ω is the soliton frequency, k is the soliton wavenumber, and ϕ_0 is the phase constant. Utilizing Eqs. (5, 6) and their derivatives, Eq. (3) transforms to:

$$\begin{aligned} & \left[-i\gamma U_1' - \omega U_1 \right] + ia_1 \left[U_1' - kiU_1 \right] + a_2 \left[U_1'' - 2ikU_1' - k^2U_1 \right] + ia_3 \left[U_1^{(3)} - 3ikU_1' - 3k^2U_1'' + ik^3U_1 \right] \\ & + a_4 \left[U_1^{(4)} - 4ikU_1^{(3)} - 6k^2U_1'' + 4ik^3U_1' + k^4U_1 \right] + ia_5 \left[U_1^{(5)} - 5ikU_1^{(4)} - 10k^2U_1^{(3)} + 10ik^3U_1'' + 5k^4U_1' - ik^5U_1 \right] \\ & + a_6 \left[U_1^{(6)} - 6ikU_1^{(5)} - 15k^2U_1^{(4)} + 20ik^3U_1^{(3)} + 15k^4U_1'' - 6ik^5U_1' - k^6U_1 \right] + (c_1U_1^2 + c_2U_2^2)U_1 = 0. \end{aligned} \quad (7)$$

In the case of Eq. (4), it changes to:

$$\begin{aligned} & \left[-i\gamma U_2' - \omega U_2 \right] + ib_1 \left[U_2' - kiU_2 \right] + b_2 \left[U_2'' - 2ikU_2' - k^2U_2 \right] + ib_3 \left[U_2^{(3)} - 3ikU_2'' - 3k^2U_2' + ik^3U_2 \right] \\ & + b_4 \left[U_2^{(4)} - 4ikU_2^{(3)} - 6k^2U_2'' + 4ik^3U_2' + k^4U_2 \right] + ib_5 \left[U_2^{(5)} - 5ikU_2^{(4)} - 10k^2U_2^{(3)} + 10ik^3U_2'' + 5k^4U_2' - ik^5U_2 \right] \\ & + b_6 \left[U_2^{(6)} - 6ikU_2^{(5)} - 15k^2U_2^{(4)} + 20ik^3U_2^{(3)} + 15k^4U_2'' - 6ik^5U_2' - k^6U_2 \right] + (d_1U_2^2 + d_2U_1^2)U_2 = 0. \end{aligned} \quad (8)$$

Eq. (7) separates into real and imaginary parts, which are:

$$\begin{aligned} & (-\omega + a_1k - a_2k^2 - a_3k^3 + a_4k^4 + a_5k^5 - a_6k^6)U_1 + (a_2 + 3a_3k - 6a_4k^2 - 10a_5k^3 + 15a_6k^4)U_1' \\ & + (a_4 + 5a_5k - 15a_6k^2)U_1^{(4)} + a_6U_1^{(6)} + (c_1U_1^3 + c_2U_1U_2^2) = 0, \end{aligned} \quad (9)$$

and

$$\begin{aligned} & \{-\gamma + a_1 - 2a_2k - 3a_3k^2 + 4a_4k^3 + 5a_5k^4 - 6a_6k^5\}U_1' + \{a_3 - 4a_4k - 10a_5k^2 + 20a_6k^3\}U_1^{(3)} \\ & + \{a_5 - 6a_6k\}U_1^{(5)} = 0. \end{aligned} \quad (10)$$

The real and imaginary parts of Eq. (8) are derived as:

$$\begin{aligned}
&(-\omega + b_1k - b_2k^2 - b_3k^3 + b_4k^4 + b_5k^5 - b_6k^6)U_2 + (b_2 + 3b_3k - 6b_4k^2 - 10b_5k^3 + 15b_6k^4)U_2'' \\
&+ (b_4 + 5b_5k - 15b_6k^2)U_2^{(4)} + b_6U_2^{(6)} + (d_1U_2^3 + d_2U_2U_1^2) = 0,
\end{aligned} \tag{11}$$

and

$$\begin{aligned}
&\{-\gamma + b_1 - 2b_2k - 3b_3k^2 + 4b_4k^3 + 5b_5k^4 - 6b_6k^5\}U_2' + \{b_3 - 4b_4k - 10b_5k^2 + 20b_6k^3\}U_2^{(3)} \\
&+ \{b_5 - 6b_6k\}U_2^{(5)} = 0.
\end{aligned} \tag{12}$$

Deriving from Eq. (10), the soliton velocity is:

$$\gamma = a_1 - 2a_2k - 3a_3k^2 + 4a_4k^3 + 5a_5k^4 - 6a_6k^5. \tag{13}$$

The soliton velocity is obtained from Eq. (12), as presented below

$$\gamma = b_1 - 2b_2k - 3b_3k^2 + 4b_4k^3 + 5b_5k^4 - 6b_6k^5. \tag{14}$$

The parameter constraint arises from equating the soliton velocities γ in both (13) and (14) as follows:

$$a_1 - 2a_2k - 3a_3k^2 + 4a_4k^3 + 5a_5k^4 - 6a_6k^5 = b_1 - 2b_2k - 3b_3k^2 + 4b_4k^3 + 5b_5k^4 - 6b_6k^5, \tag{15}$$

where

$$a_3 = 4a_4k - 10a_5k^2 + 20a_6k^3, \tag{16}$$

$$b_3 = 4b_4k - 10b_5k^2 + 20b_6k^3, \tag{17}$$

$$a_5 = 6a_6k, \tag{18}$$

$$b_5 = 6b_6k. \tag{19}$$

Thus, we arrive at:

$$a_1 - 2a_2k - 8a_4k^3 + 144a_6k^5 = b_1 - 2b_2k - 8b_4k^3 + 144b_6k^5, \tag{20}$$

$$a_3 = 4k(a_4 - 10a_6k^2), \tag{21}$$

$$b_3 = 4k(b_4 - 10b_6k^2). \tag{22}$$

The coupled system of equations (4) can be simply uncoupled under the assumption

$$U_2 = \alpha U_1, \tag{23}$$

where α is a real number. Consequently, Equations (9) and (11) can be expressed as:

$$\begin{aligned} &(-\omega + a_1k - a_2k^2 - a_3k^3 + a_4k^4 + a_5k^5 - a_6k^6)U_1 + (a_2 + 3a_3k - 6a_4k^2 - 10a_5k^3 + 15a_6k^4)U_1'' \\ &+ (a_4 + 5a_5k - 15a_6k^2)U_1^{(4)} + a_6U_1^{(6)} + (c_1 + c_2\lambda^2)U_1^3 = 0, \end{aligned} \quad (24)$$

and

$$\begin{aligned} &(-\omega + b_1k - b_2k^2 - b_3k^3 + b_4k^4 + b_5k^5 - b_6k^6)\lambda U_1 + (b_2 + 3b_3k - 6b_4k^2 - 10b_5k^3 + 15b_6k^4)\lambda U_1'' \\ &+ (b_4 + 5b_5k - 15b_6k^2)\lambda U_1^{(4)} + \lambda b_6U_1^{(6)} + (d_1\lambda^2 + d_2)\alpha U_1^3 = 0, \end{aligned} \quad (25)$$

where

$$\begin{aligned} &\frac{(-\omega + a_1k - a_2k^2 - a_3k^3 + a_4k^4 + a_5k^5 - a_6k^6)}{(-\omega + b_1k - b_2k^2 - b_3k^3 + b_4k^4 + b_5k^5 - b_6k^6)} \\ &= \frac{(a_2 + 3a_3k - 6a_4k^2 - 10a_5k^3 + 15a_6k^4)}{(b_2 + 3b_3k - 6b_4k^2 - 10b_5k^3 + 15b_6k^4)} \\ &= \frac{(a_4 + 5a_5k - 15a_6k^2)}{(b_4 + 5b_5k - 15b_6k^2)} = \frac{a_6}{b_6} = \frac{(c_1 + c_2\lambda^2)}{(d_1\lambda^2 + d_2)} = \alpha. \end{aligned}$$

4. Sardar sub-equation method (SSEM)

An important feature of the SSEM is its capability to generate a wide range of soliton solutions, including dark, bright, and singular forms, as well as complex configurations such as mixed dark-bright, dark-singular, bright-singular, and mixed singular solutions. Moreover, it provides solutions in rational, periodic, trigonometric, and various other formats.

In this method of solving Eq. (24), we proceed by assuming the solution is structured as [24]

$$U_1(\xi) = \sum_{n=0}^N \lambda_n \Psi^n(\xi), \quad \lambda_N \neq 0, \quad (26)$$

where λ_n ($n = 0, 1, \dots, N$) are constants to be determined later. The positive integer N is determined by applying the homogeneous balance method principle to Eq. (24), balancing the nonlinear term with the highest-order derivative. Additionally, the function $\Psi(\xi)$ in Eq. (26) must satisfy the following equation

$$\Psi'(\xi) = \sqrt{\eta_2 \Psi(\xi)^4 + \eta_1 \Psi(\xi)^2 + \eta_0}, \quad (27)$$

where η_l ($l = 0, 1, \dots, N$) are real constants and $\eta_2 \neq 0$. In accordance with the parameters η_l , Eq. (25) exhibits various established solutions, outlined below:

Case I Under the conditions where $\eta_0 = 0$, $\eta_1 > 0$ and $\eta_2 \neq 0$, the solutions correspond to bright and singular

solitons, respectively:

$$\Psi_{1}^{\pm}(\xi) = \pm \sqrt{-pq \left(\frac{\eta_1}{\eta_2} \right)} \operatorname{sech}_{pq} \left(\sqrt{\eta_1} \xi \right), \quad \eta_2 < 0, \quad (28)$$

and

$$\Psi_{2}^{\pm}(\xi) = \pm \sqrt{pq \left(\frac{\eta_1}{\eta_2} \right)} \operatorname{csch}_{pq} \left(\sqrt{\eta_1} \xi \right), \quad \eta_2 > 0, \quad (29)$$

where

$$\operatorname{sech}_{pq} \left(\sqrt{\eta_1} \xi \right) = \frac{2}{pe^{\sqrt{\eta_1} \xi} + qe^{-\sqrt{\eta_1} \xi}} \quad \text{and} \quad \operatorname{csch}_{pq} \left(\sqrt{\eta_1} \xi \right) = \frac{2}{pe^{\sqrt{\eta_1} \xi} - qe^{-\sqrt{\eta_1} \xi}}. \quad (30)$$

Case II When $\eta_0 = \frac{1}{4} \eta_1^2 \eta_2^2$ and $\eta_2 > 0$, $\eta_1 < 0$, we acquire the dark and singular soliton solutions, respectively:

$$\Psi_{3}^{\pm}(\xi) = \pm \sqrt{-\left(\frac{\eta_1}{2\eta_2} \right)} \operatorname{tanh}_{pq} \left(\sqrt{-\frac{\eta_1}{2}} \xi \right), \quad (31)$$

and

$$\Psi_{4}^{\pm}(\xi) = \pm \sqrt{-\left(\frac{\eta_1}{2\eta_2} \right)} \operatorname{coth}_{pq} \left(\sqrt{-\frac{\eta_1}{2}} \xi \right), \quad (32)$$

where

$$\operatorname{tanh}_{pq} \left(\sqrt{\eta_1} \xi \right) = \frac{pe^{\sqrt{\eta_1} \xi} - qe^{-\sqrt{\eta_1} \xi}}{pe^{\sqrt{\eta_1} \xi} + qe^{-\sqrt{\eta_1} \xi}} \quad \text{and} \quad \operatorname{coth}_{pq} \left(\sqrt{\eta_1} \xi \right) = \frac{pe^{\sqrt{\eta_1} \xi} + qe^{-\sqrt{\eta_1} \xi}}{pe^{\sqrt{\eta_1} \xi} - qe^{-\sqrt{\eta_1} \xi}}. \quad (33)$$

5. Application of the modified sardar sub-equation method

Starting with the application of the homogeneous balance method principle between the nonlinear term $U_1^{(6)}$ and the linear term U_1^3 from Eqs. (24) and (25), our analysis leads to $N + 6 = 3N$. From this, we derive $N = 3$, thereby transforming Eq. (26) to:

$$U_1(\xi) = \lambda_0 + \lambda_1 \Psi + \lambda_2 \Psi^2 + \lambda_3 \Psi^3, \quad (34)$$

$$U_1'(\xi) = (\lambda_1 + 2\lambda_2 \Psi + 3\lambda_3 \Psi^2) \sqrt{(\eta_2 \Psi^4 + \eta_1 \Psi^2 + \eta_0)}, \quad (35)$$

$$U_1'' = (12\lambda_3 \eta_2 \Psi^5 + 6\lambda_2 \eta_2 \Psi^4 + (2\lambda_1 \eta_2 + 9\lambda_3 \eta_1) \Psi^3 + 4\lambda_2 \eta_1 \Psi^2 + (\lambda_1 \eta_1 + 6\lambda_3 \eta_0) \Psi + 2\lambda_2 \eta_0), \quad (36)$$

$$U_1^{(3)} = (60\lambda_3 \eta_2 \Psi^4 + 24\lambda_2 \eta_2 \Psi^3 + 3(2\lambda_1 \eta_2 + 9\lambda_3 \eta_1) \Psi^2 + 8\lambda_2 \eta_1 \Psi + (\lambda_1 \eta_1 + 6\lambda_3 \eta_0)) \sqrt{(\eta_2 \Psi^4 + \eta_1 \Psi^2 + \eta_0)}, \quad (37)$$

$$\begin{aligned}
U_1^{(4)} = & (360\lambda_3\eta_2^2\Psi^7 + 120\lambda_2\eta_2^2\Psi^6 + 6\eta_2(4\lambda_1\eta_2 + 68\lambda_3\eta_1)\Psi^5 + 120\lambda_2\eta_1\eta_2\Psi^4 \\
& + (252\lambda_3\eta_0\eta_2 + 20\lambda_1\eta_1\eta_2 + 81\lambda_3\eta_1^2)\Psi^3 + (16\lambda_2\eta_1\eta_1 + 72\lambda_2\eta_0\eta_2)\Psi^2 \\
& + (\lambda_1\eta_1^2 + 60\lambda_3\eta_0\eta_1 + 12\eta_0\lambda_1\eta_2)\Psi + 8\lambda_2\eta_0\eta_1), \tag{38}
\end{aligned}$$

$$\begin{aligned}
U_1^{(5)} = & (2520\lambda_3\eta_2^2\Psi^6 + 720\lambda_2\eta_2^2\Psi^5 + 30\eta_2(4\lambda_1\eta_2 + 68\lambda_3\eta_1)\Psi^4 + 480\lambda_2\eta_1\eta_2\Psi^3 \\
& + 3(252\lambda_3\eta_0\eta_2 + 20\lambda_1\eta_1\eta_2 + 81\lambda_3\eta_1^2)\Psi^2 + 2(16\lambda_2\eta_1\eta_1 + 72\lambda_2\eta_0\eta_2)\Psi \\
& + (\lambda_1\eta_1^2 + 60\lambda_3\eta_0\eta_1 + 12\eta_0\lambda_1\eta_2))\sqrt{(\eta_2\Psi^4 + \eta_1\Psi^2 + \eta_0)}, \tag{39}
\end{aligned}$$

$$\begin{aligned}
U_1^{(6)} = & \{20160\lambda_3\eta_2^3\Psi^9 + 5040\lambda_2\eta_2^3\Psi^8 + 180\eta_2^2(4\lambda_1\eta_2 + 152\eta_1)\Psi^7 + 2520\lambda_3\eta_1\eta_2^2\Psi^7 \\
& + 6720\lambda_2\eta_1\eta_2^2\Psi^6 + [6\eta_2(2772\lambda_3\eta_0\eta_2 + 20\lambda_1\eta_1\eta_2 + 81\lambda_3\eta_1^2) + 30\eta_1\eta_2(4\lambda_1\eta_2 + 68\lambda_3\eta_1) \\
& + 6\eta_2(252\lambda_3\eta_0\eta_2 + 20\lambda_1\eta_1\eta_2 + 81\lambda_3\eta_1^2) + 120\eta_1\eta_2(4\lambda_1\eta_2 + 68\lambda_3\eta_1)]\Psi^5 + [2\eta_2(736\lambda_2\eta_1^2 \\
& + 72\lambda_2\eta_0\eta_2) + 4\eta_2(16\lambda_2\eta_1\eta_1 + 72\lambda_2\eta_0\eta_2) + 480\lambda_2\eta_1^2\eta_2 + 3600\lambda_2\eta_0\eta_2^2]\Psi^4 + [2\eta_2(\lambda_1\eta_1^2 \\
& + 60\lambda_3\eta_0\eta_1 + 12\eta_0\lambda_1\eta_2) + 6\eta_1(252\lambda_3\eta_0\eta_2 + 20\lambda_1\eta_1\eta_2 + 81\lambda_3\eta_1^2) + 3\eta_1(252\lambda_3\eta_0\eta_2 \\
& + 20\lambda_1\eta_1\eta_2 + 81\lambda_3\eta_1^2) + 120\eta_0\eta_2(4\lambda_1\eta_2 + 68\lambda_3\eta_1)]\Psi^3 + [2\eta_1(16\lambda_2\eta_1\eta_1 + 72\lambda_2\eta_0\eta_2) \\
& + 1440\lambda_2\eta_0\eta_1\eta_2 + 2(16\lambda_2\eta_1^3 + 72\lambda_2\eta_0\eta_1^2\eta_2)]\Psi^2 + [\eta_1(\lambda_1\eta_1^2 + 60\lambda_3\eta_0\eta_1 + 12\eta_0\lambda_1\eta_2) \\
& + 6\eta_0(252\lambda_3\eta_0\eta_2 + 20\lambda_1\eta_1\eta_2 + 81\lambda_3\eta_1^2)]\Psi + 2\eta_0(16\lambda_2\eta_1^2 + 72\lambda_2\eta_0\eta_2)\}. \tag{40}
\end{aligned}$$

Eq. (24) can be written as:

$$M_1U_1 + M_2U_1'' + M_3U_1^{(4)} + a_6U_1^{(6)} + (c_1 + c_2\lambda^2)U_1^3 = 0, \tag{41}$$

where:

$$M_1 = (-\omega + a_1k - a_2k^2 - a_3k^3 + a_4k^4 + a_5k^5 - a_6k^6), \tag{42}$$

$$M_2 = (a_2 + 3a_3k - 6a_4k^2 - 10a_5k^3 + 15a_6k^4), \tag{43}$$

$$M_3 = (a_4 + 5a_5k - 15a_6k^2). \quad (44)$$

Substituting Eqs. (36), (38), and (40) into Eq. (41) and taking into consideration Eq. (27), we get:

$$\begin{aligned} & M_1(\lambda_0 + \lambda_1\Psi + \lambda_2\Psi^2 + \lambda_3\Psi^3) + M_2(12\lambda_3\eta_2\Psi^5 + 6\lambda_2\eta_2\Psi^4 + (2\lambda_1\eta_2 + 9\lambda_3\eta_1)\Psi^3 \\ & + 4\lambda_2\eta_1\Psi^2 + (\lambda_1\eta_1 + 6\lambda_3\eta_0)\Psi + 2\lambda_2\eta_0) + M_3(360\lambda_3\eta_2^2\Psi^7 + 120\lambda_2\eta_2^2\Psi^6 + 6\eta_2(4\lambda_1\eta_2 \\ & + 68\lambda_3\eta_1)\Psi^5 + 120\lambda_2\eta_1\eta_2\Psi^4 + (252\lambda_3\eta_0\eta_2 + 20\lambda_1\eta_1\eta_2 + 81\lambda_3\eta_1^2)\Psi^3 + (16\lambda_2\eta_1\eta_1 \\ & + 72\lambda_2\eta_0\eta_2)\Psi^2 + (\lambda_1\eta_1^2 + 60\lambda_3\eta_0\eta_1 + 12\eta_0\lambda_1\eta_2)\Psi + 8\lambda_2\eta_0\eta_1) + a_6\{20160\lambda_3\eta_2^3\Psi^9 \\ & + 5040\lambda_2\eta_2^3\Psi^8 + 180\eta_2^2(4\lambda_1\eta_2 + 152\eta_1)\Psi^7 + 2520\lambda_3\eta_1\eta_2^2\Psi^7 + 6720\lambda_2\eta_1\eta_2^2\Psi^6 \\ & + [6\eta_2(2772\lambda_3\eta_0\eta_2 + 20\lambda_1\eta_1\eta_2 + 81\lambda_3\eta_1^2) + 30\eta_1\eta_2(4\lambda_1\eta_2 + 68\lambda_3\eta_1) + 6\eta_2(252\lambda_3\eta_0\eta_2 \\ & + 20\lambda_1\eta_1\eta_2 + 81\lambda_3\eta_1^2) + 120\eta_1\eta_2(4\lambda_1\eta_2 + 68\lambda_3\eta_1)]\Psi^5 + [2\eta_2(736\lambda_2\eta_1^2 + 72\lambda_2\eta_0\eta_2) \\ & + 4\eta_2(16\lambda_2\eta_1\eta_1 + 72\lambda_2\eta_0\eta_2) + 480\lambda_2\eta_1^2\eta_2 + 3600\lambda_2\eta_0\eta_2^2]\Psi^4 + [2\eta_2(\lambda_1\eta_1^2 + 60\lambda_3\eta_0\eta_1 + \\ & + 12\eta_0\lambda_1\eta_2) + 6\eta_1(252\lambda_3\eta_0\eta_2 + 20\lambda_1\eta_1\eta_2 + 81\lambda_3\eta_1^2) + 3\eta_1(252\lambda_3\eta_0\eta_2 + 20\lambda_1\eta_1\eta_2 \\ & + 81\lambda_3\eta_1^2) + 120\eta_0\eta_2(4\lambda_1\eta_2 + 68\lambda_3\eta_1)]\Psi^3 + [2\eta_1(16\lambda_2\eta_1\eta_1 + 72\lambda_2\eta_0\eta_2) + 1440\lambda_2\eta_0\eta_1\eta_2 \\ & + 2(16\lambda_2\eta_1^3 + 72\lambda_2\eta_0\eta_1\eta_2)]\Psi^2 + [\eta_1(\lambda_1\eta_1^2 + 60\lambda_3\eta_0\eta_1 + 12\eta_0\lambda_1\eta_2) + 6\eta_0(252\lambda_3\eta_0\eta_2 \\ & + 20\lambda_1\eta_1\eta_2 + 81\lambda_3\eta_1^2)]\Psi + 2\eta_0(16\lambda_2\eta_1^2 + 72\lambda_2\eta_0\eta_2)\} + (c_1 + c_2\lambda^2)(\lambda_0 + \lambda_1\Psi + \lambda_2\Psi^2 + \lambda_3\Psi^3)^3 = 0. \quad (45) \end{aligned}$$

Upon collecting and equating the coefficients of the independent functions $\Psi^j(\xi)$ to zero, we obtain the following outcomes:

Case I With $\eta_0 = 0$, $\lambda_0 = 0$, $\lambda_1 = 0$, Eq. (45) reduces to the following equation:

$$\begin{aligned}
& M_1(\lambda_2 \Psi^2 + \lambda_3 \Psi^3) + M_2(12\lambda_3 \eta_2 \Psi^5 + 6\lambda_2 \eta_2 \Psi^4 + 9\lambda_3 \eta_1 \Psi^3 + 4\lambda_2 \eta_1 \Psi^2) + M_3(360\lambda_3 \eta_2^2 \Psi^7 \\
& + 120\lambda_2 \eta_2^2 \Psi^6 + 408\lambda_3 \eta_1 \eta_2 \Psi^5 + 120\lambda_2 \eta_1 \eta_2 \Psi^4 + 81\lambda_3 \eta_1^2 \Psi^3 + 16\lambda_2 \eta_1^2 \Psi^2) \\
& + a_6 \{20160\lambda_3 \eta_2^3 \Psi^9 + 5040\lambda_2 \eta_2^3 \Psi^8 + 29880\lambda_3 \eta_1 \eta_2^2 \Psi^7 + 6720\lambda_2 \eta_1 \eta_2^2 \Psi^6 \\
& + 11172\lambda_3 \eta_1^2 \eta_2 \Psi^5 + 2016\lambda_2 \eta_1^2 \eta_2 \Psi^4 + 729\lambda_3 \eta_1^3 \Psi^3 + 64\lambda_2 \eta_1^3 \Psi^2\} + (c_1 + c_2 \lambda^2) \\
& (\lambda_2^3 \Psi^6 + 3\lambda_2^2 \lambda_3 \Psi^7 + 3\lambda_3^2 \lambda_2 \Psi^8 + \lambda_3^3 \Psi^9) = 0.
\end{aligned} \tag{46}$$

To find the coefficients of Ψ^j for $j = 2, 3, 4, 5, 6, 7, 8, 9$, we set up the system of algebraic equations by equating them to zero:

$$\begin{aligned}
\Psi^9 : 20160a_6 \eta_2^3 + (c_1 + c_2 \lambda^2) \lambda_3^2 &= 0, \\
\Psi^8 : 1680a_6 \eta_2^3 + (c_1 + c_2 \lambda^2) \lambda_3^2 &= 0, \\
\Psi^7 : 120M_3 \eta_2^2 + 9960a_6 \eta_1 \eta_2^2 + (c_1 + c_2 \lambda^2) \lambda_2^2 &= 0, \\
\Psi^6 : 120\eta_2^2 M_3 + a_6 6720 \eta_1 \eta_2^2 + (c_1 + c_2 \lambda^2) \lambda_2^2 &= 0, \\
\Psi^5 : M_2 + 34M_3 \eta_1 + 931a_6 \eta_1^2 &= 0, \\
\Psi^4 : M_2 + 20M_3 \eta_1 + 336a_6 \eta_1^2 &= 0, \\
\Psi^3 : M_1 + M_2 9 \eta_1 + M_3 81 \eta_1^2 + a_6 729 \eta_1^3 &= 0, \\
\Psi^2 : M_1 + M_2 4 \eta_1 + M_3 16 \eta_1^2 + a_6 64 \eta_1^3 &= 0.
\end{aligned} \tag{47}$$

The solution to the system of algebraic equations (47) provides us with the soliton wavenumber

$$\omega = a_1 k - a_2 k^2 - a_3 k^3 + a_4 k^4 + a_5 k^5 - a_6 k^6, \tag{48}$$

and the corresponding bright and singular soliton solutions, respectively:

$$\begin{aligned}
u_{1,a}(x, t) &= \left(-pq \frac{\eta_1}{\eta_2} \right) \left[\lambda_2 \operatorname{sech}^2 p_q \left(\sqrt{\eta_1} (x - \gamma t) \right) + \lambda_3 \sqrt{\left(-pq \frac{\eta_1}{\eta_2} \right)} \operatorname{sech}^3 p_q \left(\sqrt{\eta_1} (x - \gamma t) \right) \right] \\
&\exp \left[i(-\kappa x + \omega t + \theta_0) \right], \quad \eta_2 < 0,
\end{aligned} \tag{49}$$

$$u_{1,b}(x, t) = \left(-pq \frac{\eta_1}{\eta_2}\right) \left[\lambda_2 \operatorname{csch}_{pq}^2(\sqrt{\eta_1}(x-\gamma t)) + \lambda_3 \sqrt{\left(-pq \frac{\eta_1}{\eta_2}\right)} \operatorname{csch}_{pq}^3(\sqrt{\eta_1}(x-\gamma t)) \right] \exp[i(-\kappa x + \omega t + \theta_0)], \quad \eta_2 < 0, \quad (50)$$

$$v_{1,a}(x, t) = \alpha \left(-pq \frac{\eta_1}{\eta_2}\right) \left[\lambda_2 \operatorname{sech}_{pq}^2(\sqrt{\eta_1}(x-\gamma t)) + \lambda_3 \sqrt{\left(-pq \frac{\eta_1}{\eta_2}\right)} \operatorname{sech}_{pq}^3(\sqrt{\eta_1}(x-\gamma t)) \right] \exp[i(-\kappa x + \omega t + \theta_0)], \quad \eta_2 < 0, \quad (51)$$

$$v_{1,b}(x, t) = \alpha \left(pq \frac{\eta_1}{\eta_2}\right) \left[\lambda_2 \operatorname{csch}_{pq}^2(\sqrt{\eta_1}(x-\gamma t)) + \lambda_3 \sqrt{\left(pq \frac{\eta_1}{\eta_2}\right)} \operatorname{csch}_{pq}^3(\sqrt{\eta_1}(x-\gamma t)) \right] \exp[i(-\kappa x + \omega t + \theta_0)], \quad \eta_2 < 0, \quad (52)$$

where the parametric constraints are defined as follows:

Family 1

$$\eta_1 = -\frac{M_3}{13a_6}, \quad \lambda_2 = \sqrt{\frac{646M_3}{(c_1 + c_2\lambda^2)}}\eta_2, \quad \lambda_3 = \mp \sqrt{-\frac{20160a_6\eta_2}{(c_1 + c_2\lambda^2)}}\eta_2. \quad (53)$$

Family 2

$$\eta_1 = -\frac{M_3}{13a_6}, \quad \lambda_2 = \sqrt{\frac{646M_3}{(c_1 + c_2\lambda^2)}}\eta_2, \quad \lambda_3 = \mp \sqrt{-\frac{1680a_6\eta_2}{(c_1 + c_2\lambda^2)}}\eta_2. \quad (54)$$

Family 3

$$\eta_1 = -\frac{M_3}{13a_6}, \quad \lambda_2 = \sqrt{\frac{397M_3}{(c_1 + c_2\lambda^2)}}\eta_2, \quad \lambda_3 = \mp \sqrt{-\frac{20160a_6\eta_2}{(c_1 + c_2\lambda^2)}}\eta_2. \quad (55)$$

Family 4

$$\eta_1 = -\frac{M_3}{13a_6}, \quad \lambda_2 = \sqrt{\frac{397M_3}{(c_1 + c_2\lambda^2)}}\eta_2, \quad \lambda_3 = \mp \sqrt{-\frac{1680a_6\eta_2}{(c_1 + c_2\lambda^2)}}\eta_2. \quad (56)$$

Family 5

$$\eta_1 = -\frac{M_3}{42.5a_6}, \quad \lambda_2 = \sqrt{\frac{38M_3}{(c_1 + c_2\lambda^2)}}\eta_2, \quad \lambda_3 = \mp \sqrt{-\frac{20160a_6\eta_2}{(c_1 + c_2\lambda^2)}}\eta_2. \quad (57)$$

Family 6

$$\eta_1 = -\frac{M_3}{42.5a_6}, \lambda_2 = \sqrt{\frac{38M_3}{(c_1 + c_2\lambda^2)}}\eta_2, \lambda_3 = \mp \sqrt{-\frac{1680a_6\eta_2}{(c_1 + c_2\lambda^2)}}\eta_2. \quad (58)$$

Family 7

$$\eta_1 = -\frac{M_3}{42.5a_6}, \lambda_2 = \sqrt{\frac{214M_3}{(c_1 + c_2\lambda^2)}}\eta_2, \lambda_3 = \mp \sqrt{-\frac{20160a_6\eta_2}{(c_1 + c_2\lambda^2)}}\eta_2. \quad (59)$$

Family 8

$$\eta_1 = -\frac{M_3}{42.5a_6}, \lambda_2 = \sqrt{\frac{214M_3}{(c_1 + c_2\lambda^2)}}\eta_2, \lambda_3 = \mp \sqrt{-\frac{1680a_6\eta_2}{(c_1 + c_2\lambda^2)}}\eta_2. \quad (60)$$

Case II Under the condition $\eta_0 = \frac{1}{4} \frac{\eta_1^2}{\eta_2}$, $\lambda_0 = 0$, $\lambda_1 = 0$, $\lambda_2 = 0$, $\eta_2 > 0$ Eq. (45) can be rewritten as:

$$M_1\Psi^3 + M_2\left(12\eta_2\Psi^5 + 9\eta_1\Psi^3 + \frac{3}{2}\frac{\eta_1^2}{\eta_2}\Psi\right) + M_3\left(360\eta_2^2\Psi^7 + 408\eta_1\eta_2\Psi^5 + 144\eta_1^2\Psi^3 + 15\left(\frac{\eta_1^3}{\eta_2}\right)\Psi\right) + a_6\left\{\left(20160\eta_2^3 + (c_1 + c_2\alpha^2)\lambda_3^2\right)\Psi^9 + 29880\eta_1\eta_2^2\Psi^7 + 15708\eta_2\eta_1^2\Psi^5 + 3366\eta_1^3\Psi^3 + 231\frac{\eta_1^4}{\eta_2}\Psi\right\} = 0. \quad (61)$$

We formulate a system of algebraic equations to find the coefficients of Ψ^j for $j = 1, 2, 3, 4, 5, 6, 7, 8, 9$, equating them to zero:

$$\begin{aligned} \Psi^9 : 20160\eta_2^3 + (c_1 + c_2\alpha^2)\lambda_3^2 &= 0, \\ \Psi^7 : M_3 + 83a_6\eta_1 &= 0, \\ \Psi^5 : M_2 + 34M_3\eta_1 + 1309a_6\eta_1^2 &= 0, \\ \Psi^3 : M_1 + 9\eta_1M_2 + 144\eta_1^2M_3 + 3366\eta_1^3a_6 &= 0, \\ \Psi : M_2 + 10M_3\eta_1 + 154a_6\eta_1^2 &= 0. \end{aligned} \quad (62)$$

Solving the system of algebraic equations (62) yields the soliton wavenumber

$$\omega = k(a_1 - a_2k - 3a_4k^3 - 35a_6k^5), \quad (63)$$

as well as the dark and singular soliton solutions, respectively:

$$u_{2,a}(x, t) = \sqrt{\left(\frac{-\eta_1}{2\eta_2}\right)^3} \lambda_3 \tanh^3_{pq} \left(\sqrt{\frac{-\eta_1}{2}}(x - \gamma t) \right) \exp[i(-\kappa x + \omega t + \theta_0)], \eta_2 > 0, \quad (64)$$

$$u_{2,b}(x, t) = \sqrt{\left(\frac{-\eta_1}{2\eta_2}\right)^3} \lambda_3 \coth^3_{pq} \left(\sqrt{\frac{-\eta_1}{2}}(x - \gamma t) \right) \exp[i(-\kappa x + \omega t + \theta_0)], \eta_2 > 0, \quad (65)$$

$$v_{2,a}(x, t) = \alpha \sqrt{\left(\frac{-\eta_1}{2\eta_2}\right)^3} \lambda_3 \tanh^3_{pq} \left(\sqrt{\frac{-\eta_1}{2}}(x - \gamma t) \right) \exp[i(-\kappa x + \omega t + \theta_0)], \eta_2 > 0, \quad (66)$$

$$v_{2,b}(x, t) = \alpha \sqrt{\left(\frac{-\eta_1}{2\eta_2}\right)^3} \lambda_3 \coth^3_{pq} \left(\sqrt{\frac{-\eta_1}{2}}(x - \gamma t) \right) \exp[i(-\kappa x + \omega t + \theta_0)], \eta_2 > 0, \quad (67)$$

where the parameters are constrained by:

Family 1

$$\eta_0 = \frac{1}{4} \frac{\eta_1^2}{\eta_2}, \lambda_3 = \sqrt{\frac{-20160\eta_2}{(c_1 + c_2\alpha^2)}} \eta_2, a_6 \neq 0, \eta_1 = -\frac{M_3}{83a_6}. \quad (68)$$

Family 2

$$\eta_0 = \frac{1}{4} \frac{\eta_1^2}{\eta_2}, \lambda_3 = \sqrt{\frac{-20160\eta_2}{(c_1 + c_2\alpha^2)}} \eta_2, a_6 \neq 0, \eta_1 = \frac{-17M_3 \mp \sqrt{289M_3^2 - (1309a_6)M_2}}{1309a_6}, 289M_3^2 > (1309a_6)M_2. \quad (69)$$

Family 3

$$\eta_0 = \frac{1}{4} \frac{\eta_1^2}{\eta_2}, \lambda_3 = \sqrt{\frac{-20160\eta_2}{(c_1 + c_2\alpha^2)}} \eta_2, a_6 \neq 0, \eta_1 = \frac{-8M_3 \mp \sqrt{64M_3^2 - (374a_6)M_2}}{374a_6}, 64M_3^2 > (374a_6)M_2. \quad (70)$$

Family 4

$$\eta_0 = \frac{1}{4} \frac{\eta_1^2}{\eta_2}, \lambda_3 = \sqrt{\frac{-20160\eta_2}{(c_1 + c_2\alpha^2)}} \eta_2, a_6 \neq 0, \eta_1 = \frac{-5M_3 \mp \sqrt{25M_3^2 - (154a_6)M_2}}{154a_6}, 25M_3^2 > (154a_6)M_2. \quad (71)$$

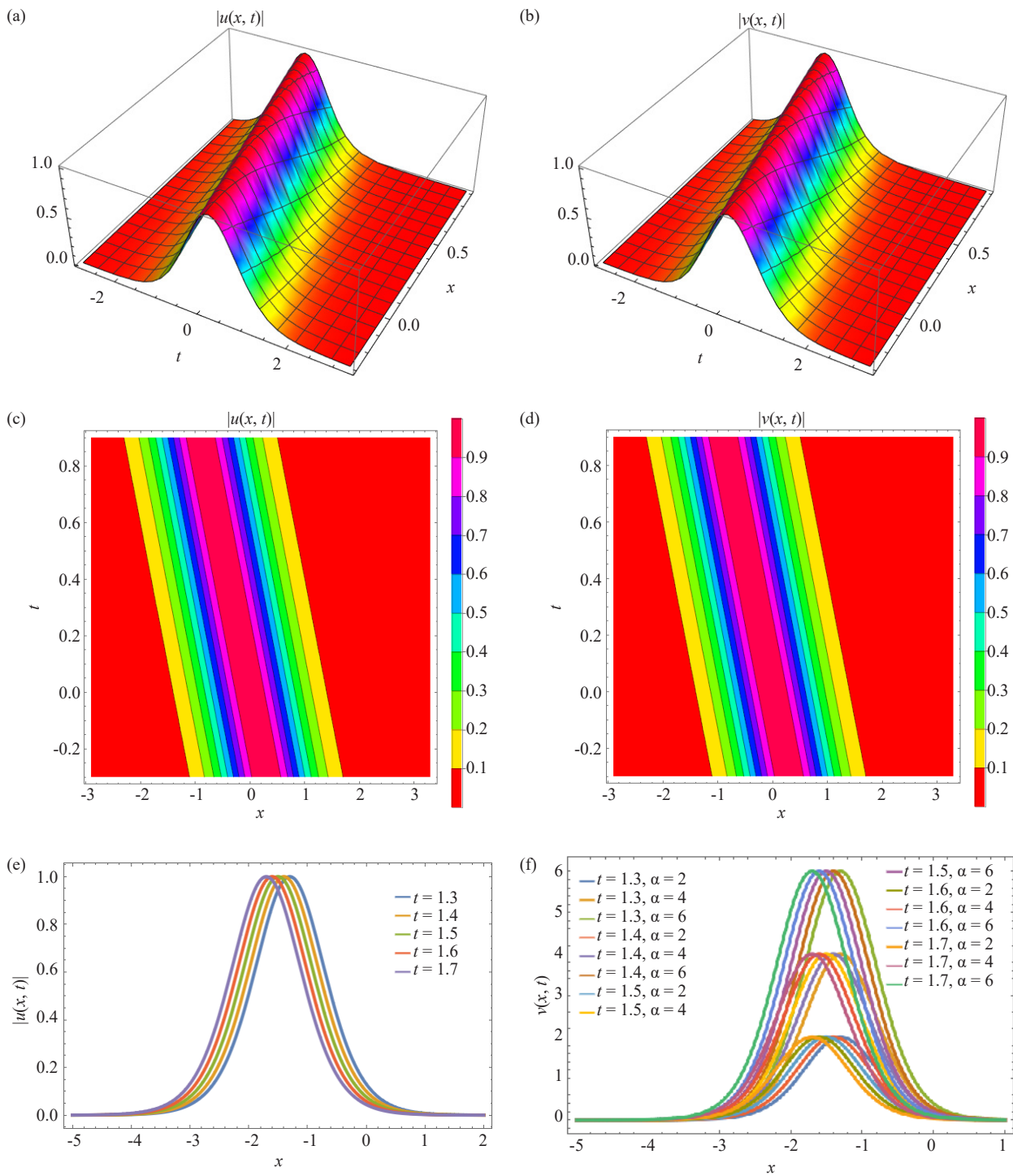


Figure 1. Profile of bright soliton solutions; (a) Surface plot; (b) Surface plot; (c) Contour plot; (d) Contour plot; (e) 2D plot; (f) 2D plot

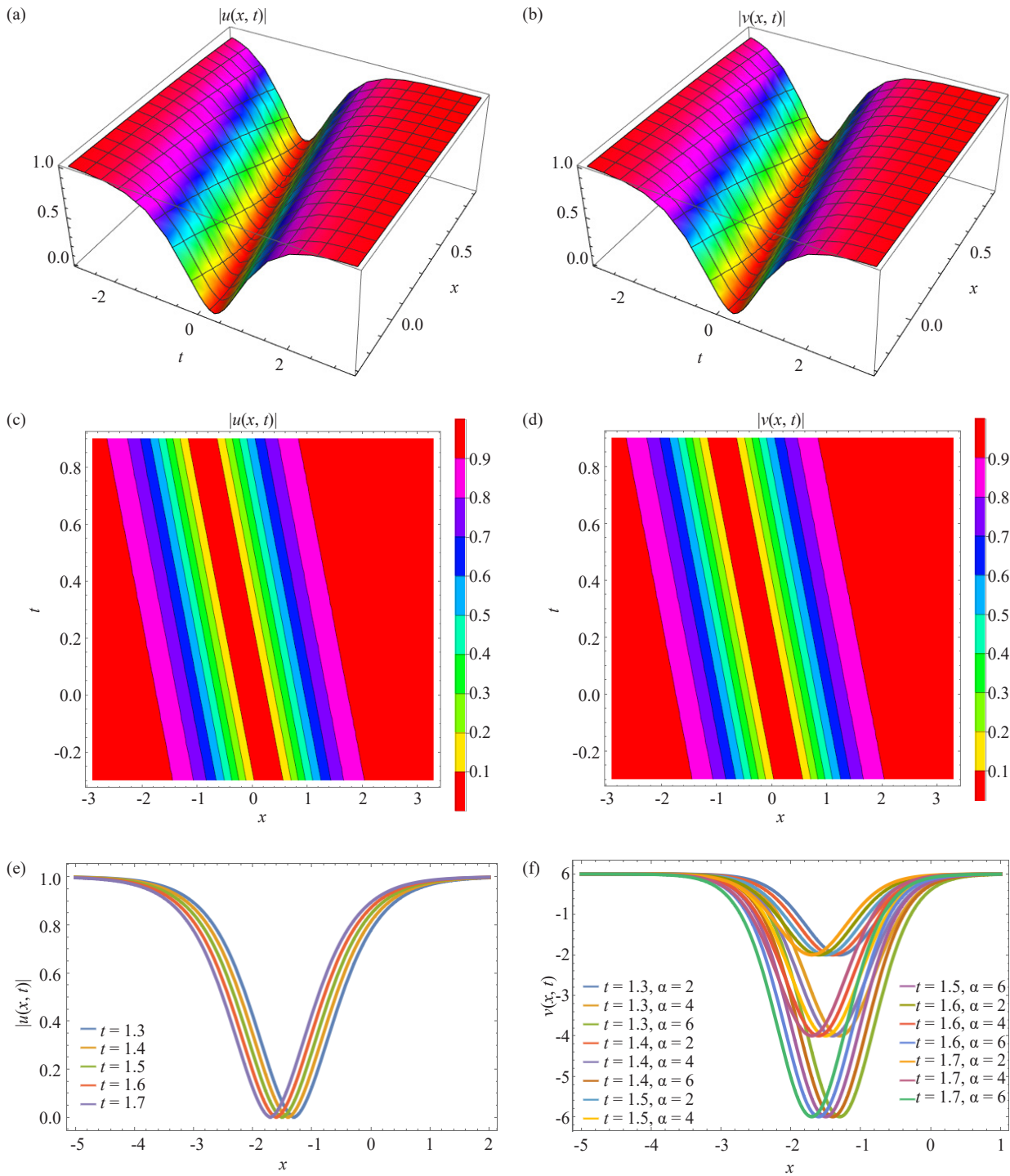


Figure 2. Profile of dark soliton solutions; (a) Surface plot; (b) Surface plot; (c) Contour plot; (d) Contour plot; (e) 2D plot; (f) 2D plot

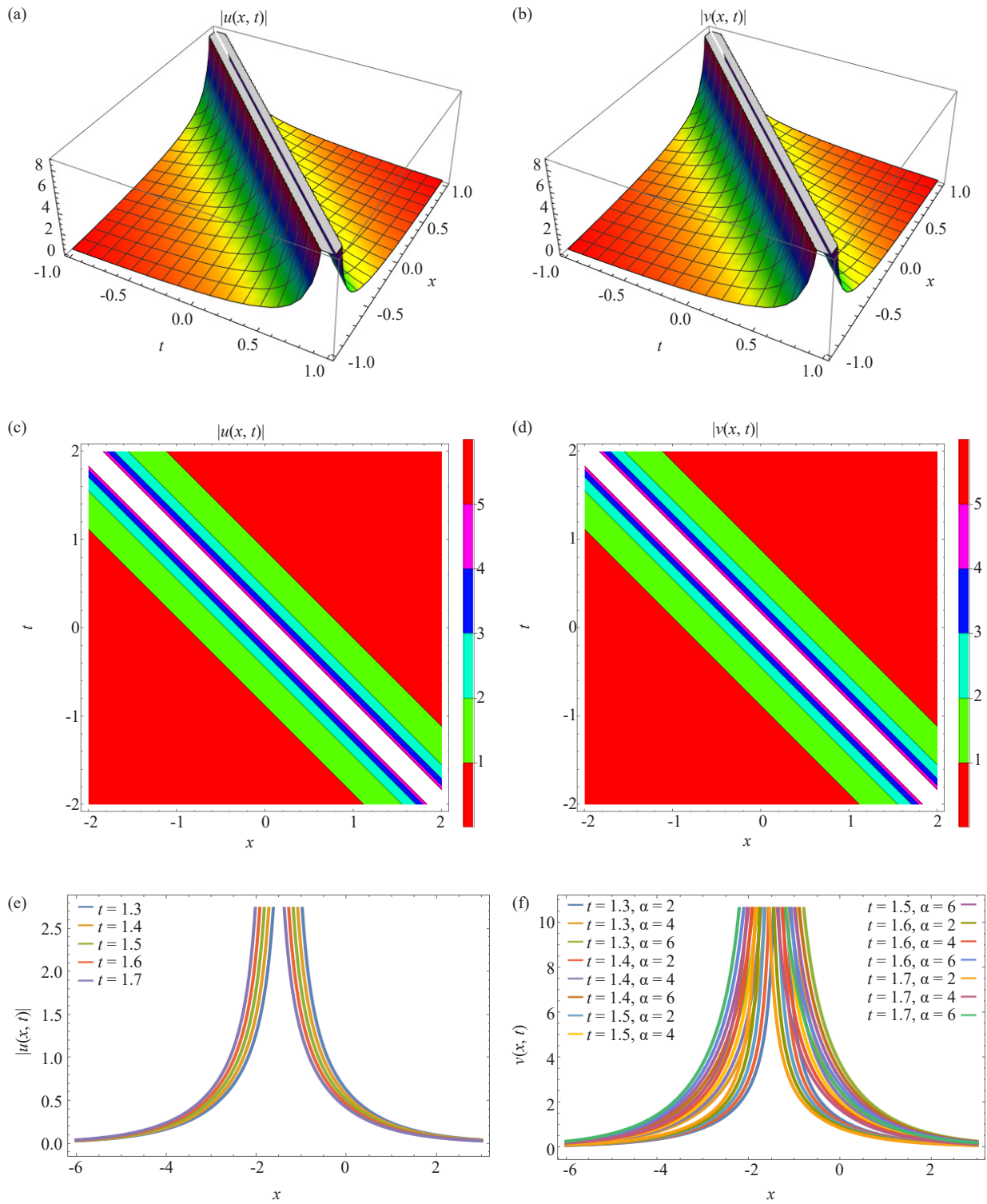


Figure 3. Profile of singular soliton solutions; (a) Surface plot; (b) Surface plot; (c) Contour plot; (d) Contour plot; (e) 2D plot; (f) 2D plot

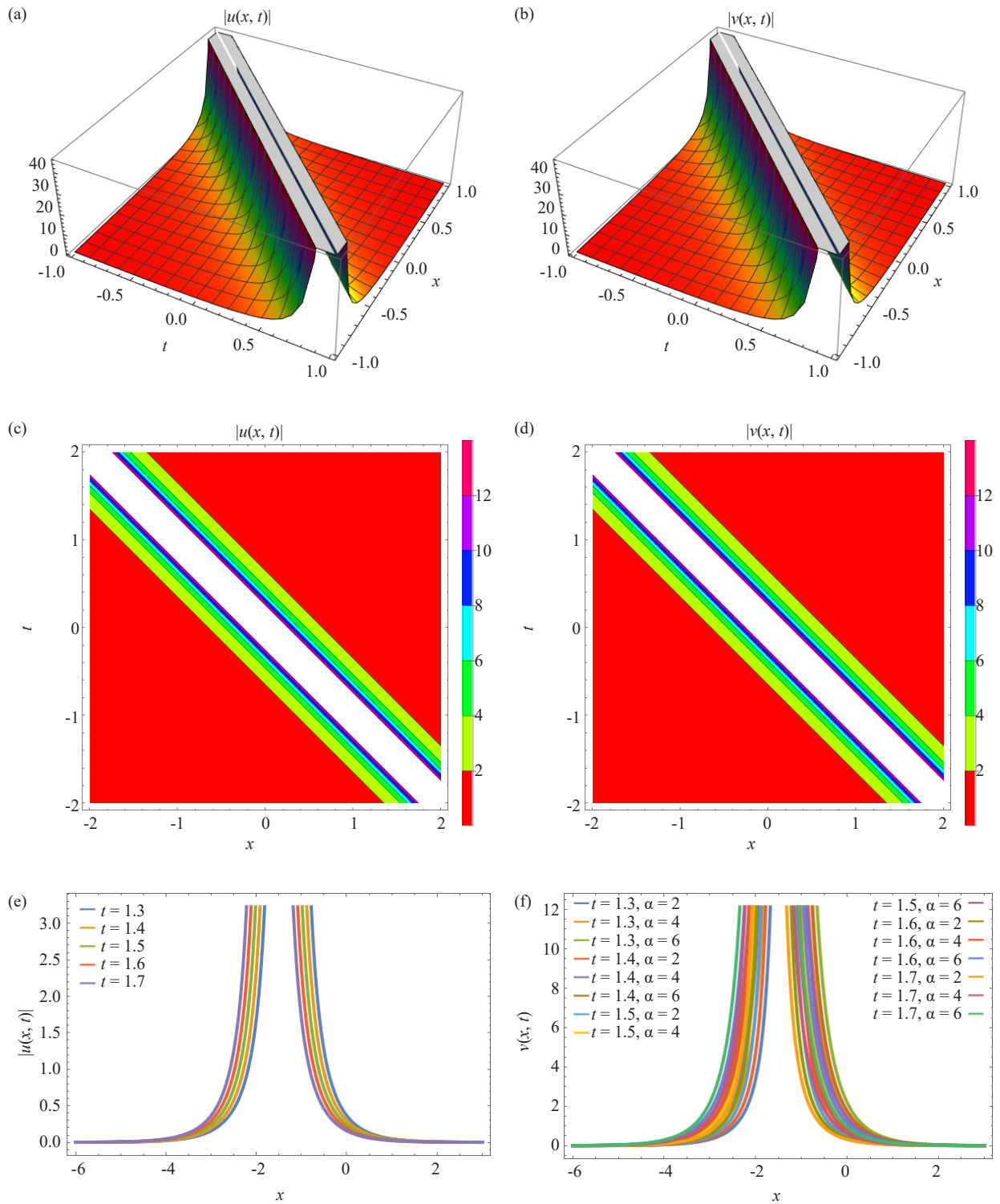


Figure 4. Profile of singular soliton solutions; (a) Surface plot; (b) Surface plot; (c) Contour plot; (d) Contour plot; (e) 2D plot; (f) 2D plot

6. Results and discussion

Figure 1 illustrates the behavior of bright soliton solutions $u(x, t)$ and $v(x, t)$ through various visualizations, including surface plots, contour plots, and 2D plots. The bright soliton solutions are derived from the complex-valued

expressions (49) and (51) along with (53). The parameters are set as $t = 1.3, 1.4, 1.5, 1.6, 1.7$ and $\alpha = 2, 4, 6$, with specific values for other parameters: $a_1 = 1, a_2 = 1, a_3 = 1, a_4 = 1, a_5 = 1, a_6 = -1, b_1 = 1, b_2 = 1, b_3 = 1, b_4 = 1, b_5 = 1, b_6 = -1, c_1 = 1, c_2 = 1, \lambda = 1, k = 1, p = 1, q = 1$ and $\eta_2 = -1$. Figures 1(a) and 1(b) depict the evolution of bright solitons in three-dimensional space. The solitons maintain their shape and peak intensity over time, characteristic of bright solitons which are localized pulses that do not disperse. The surface plots clearly show the stability and persistence of these solitons as t increases. Figures 1(c) and 1(d) provide a two-dimensional view of the soliton intensity distribution over the x and t plane. The bright soliton contours display high-intensity regions, corresponding to the soliton peaks, surrounded by lower-intensity areas. These plots emphasize the localized nature of bright solitons. Figure 1(e) shows the soliton profiles at different time instances, demonstrating how the solitons maintain their peak amplitude and shape. Figure 1(f) explores the effect of varying the parameter α , revealing that changes in α alter the width and amplitude of the solitons. Higher values of α result in narrower and taller solitons, indicating a direct relationship between α and the soliton's properties. Figure 2 presents the dark soliton solutions $u(x, t)$ and $v(x, t)$, derived from the complex-valued expressions (64) and (66) along with (68). The dark soliton solutions are characterized by a localized dip in an otherwise continuous wave background. Figures 2(a) and 2(b) illustrate the evolution of dark solitons over time. Unlike bright solitons, dark solitons appear as depressions or dips in the wave profile. These plots show the stability of the dark solitons and their persistence over time. Figures 2(c) and 2(d) highlight the intensity distribution of dark solitons. The dark solitons are represented by low-intensity regions within a continuous background, emphasizing their nature as dips in the wave amplitude. Figure 2(e) shows the soliton profiles at different time instances, indicating that the depth and width of the solitons remain consistent over time. Figure 2(f) examines the effect of varying α , showing that higher values of α increase the depth and decrease the width of the solitons. This relationship highlights how α influences the properties of dark solitons. Figures 3 and 4 display the singular soliton solutions $u(x, t)$ and $v(x, t)$, derived from the complex-valued expressions (50) and (52) via (53) for Figure 3, and (65) and (67) via (68) for Figure 4. Singular solitons are characterized by their unique profiles which may include singularities or infinite peaks. Figures 3(a), 3(b), 4(a), and 4(b) demonstrate the evolution of singular solitons. These solitons exhibit sharp peaks or singularities that remain stable over time. The plots highlight the distinct nature of singular solitons compared to bright and dark solitons. Figures 3(c), 3(d), 4(c), and 4(d) for singular solitons show regions of very high intensity, corresponding to the singular peaks. These plots emphasize the unique characteristics of singular solitons, with contours sharply focusing around the singularities. Figure 3(e) and 4(e) show the soliton profiles over time, illustrating the persistence of the singularity. Figure 3(f) and 4(f) explore the effect of α , revealing that changes in α significantly impact the shape and intensity of the singularities. Higher α values result in more pronounced singularities, indicating a strong dependence of singular soliton properties on α . The figures collectively highlight the distinct characteristics of bright, dark, and singular soliton solutions. Bright solitons are localized peaks that maintain their shape over time, while dark solitons are localized dips in a continuous wave background. Singular solitons exhibit unique profiles with singularities or infinite peaks. The effect of the parameter α is significant across all types of solitons, influencing their width, amplitude, and overall shape. These visualizations provide valuable insights into the dynamics and stability of different soliton solutions under varying conditions.

7. Conclusion

The paper recovered highly dispersive optical soliton solutions for the NLSE with Kerr law of SPM with polarization-mode dispersion. The integration scheme, Sardar's sub-equation method, was implemented. Thus a complete picture of soliton solutions is obtained. The results are interesting in the sense that future holds strong for the model. Later the model will be studied after extending it to dispersion-flattened fibers. This would give a complete picture with highly dispersive optical solitons. The results of such research activities are awaited at the current moment and will be made available and aligned with the pre-existing works [21-29].

Conflict of interest

The authors declare that they have no known competing financial interests or personal relationships that could have appeared to influence the work reported in this paper.

References

- [1] Sağlam Özkan Y, Yaşar E. Three efficient schemes and highly dispersive optical solitons of perturbed Fokas-Lenells equation in stochastic form. *Ukrainian Journal of Physical Optics*. 2024; 25(5): S1038.
- [2] Wazwaz AM, Alhejaili W, El-Tantawy SA. Optical solitons for nonlinear Schrödinger equation formatted in the absence of chromatic dispersion through modified exponential rational function method and other distinct schemes. *Ukrainian Journal of Physical Optics*. 2024; 25(5): S1059.
- [3] Li N, Chen Q, Triki H, Liu F, Sun Y, Xu S, et al. Bright and dark solitons in a (2+1)-dimensional spin-1 Bose-Einstein condensates. *Ukrainian Journal of Physical Optics*. 2024; 25(5): S1074.
- [4] Gao X, Shi J, Belić MR, Chen J, Li J, Zeng L, et al. W-shaped solitons under inhomogeneous self-defocusing Kerr nonlinearity. *Ukrainian Journal of Physical Optics*. 2024; 25(5): S1085.
- [5] Dakova-Mollova A, Miteva P, Slavchev V, Kovachev K, Kasapeteva Z, Dakova D, et al. Propagation of broad-band optical pulses in dispersionless media. *Ukrainian Journal of Physical Optics*. 2024; 25(5): S1110.
- [6] Wazwaz AM. Pure-quartic stationary optical bullets for (3+1)-dimensional nonlinear Schrödinger's equation with fourth-order dispersive effects and parabolic law of nonlinearity. *Ukrainian Journal of Physical Optics*. 2024; 25(5): S1136.
- [7] Xu SY, Yang AC, Zhou Q. Prediction of nondegenerate solitons and parameters in nonlinear birefringent optical fibers using PhPINN and DeepONet algorithms. *Ukrainian Journal of Physical Optics*. 2024; 25(5): S1150.
- [8] Wang S. Novel soliton solutions of CNLSEs with Hirota bilinear method. *Journal of Optics*. 2023; 52(3): 1602-1607.
- [9] Kopçasız B, Yaşar E. The investigation of unique optical soliton solutions for dual-mode nonlinear Schrödinger's equation with new mechanisms. *Journal of Optics*. 2023; 52(3): 1513-1527.
- [10] Tang L. Bifurcations and optical solitons for the coupled nonlinear Schrödinger equation in optical fiber Bragg gratings. *Journal of Optics*. 2023; 52(3): 1388-1398.
- [11] Thi TN, Van LC. Supercontinuum generation based on suspended core fiber infiltrated with butanol. *Journal of Optics*. 2023; 52(4): 2296-2305.
- [12] Li Z, Zhu E. Optical soliton solutions of stochastic Schrödinger-Hirota equation in birefringent fibers with spatiotemporal dispersion and parabolic law nonlinearity. *Journal of Optics*. 2024; 53(2): 1302-1308.
- [13] Han T, Li Z, Li C, Zhao L. Bifurcations, stationary optical solitons and exact solutions for complex Ginzburg-Landau equation with nonlinear chromatic dispersion in non-Kerr law media. *Journal of Optics*. 2023; 52(2): 831-844.
- [14] Tang L. Phase portraits and multiple optical solitons perturbation in optical fibers with the nonlinear Fokas-Lenells equation. *Journal of Optics*. 2023; 52(4): 2214-2223.
- [15] Nandy S, Lakshminarayanan V. Adomian decomposition of scalar and coupled nonlinear Schrödinger equations and dark and bright solitary wave solutions. *Journal of Optics*. 2015; 44: 397-404.
- [16] Chen W, Shen M, Kong Q, Wang Q. The interaction of dark solitons with competing nonlocal cubic nonlinearities. *Journal of Optics*. 2015; 44: 271-280.
- [17] Xu SL, Petrović N, Belić MR. Two-dimensional dark solitons in diffusive nonlocal nonlinear media. *Journal of Optics*. 2015; 44: 172-177.
- [18] Dowluru RK, Bhima PR. Influences of third-order dispersion on linear birefringent optical soliton transmission systems. *Journal of Optics*. 2011; 40: 132-142.
- [19] Singh M, Sharma AK, Kaler RS. Investigations on optical timing jitter in dispersion managed higher order soliton system. *Journal of Optics*. 2011; 40: 1-7.
- [10] Janyani V. Formation and propagation-dynamics of primary and secondary soliton-like pulses in bulk nonlinear media. *Journal of Optics*. 2008; 37: 1-8.
- [21] Hasegawa A. Application of optical solitons for information transfer in fibers-A tutorial review. *Journal of Optics*. 2004; 33(3): 145-156.
- [22] Mahalingam A, Uthayakumar A, Anandhi P. Dispersion and nonlinearity managed multisoliton propagation in an

- erbium doped inhomogeneous fiber with gain/loss. *Journal of Optics*. 2013; 42: 182-188.
- [23] AlQahtani SA, Alngar ME, Shohib R, Alawwad AM. Enhancing the performance and efficiency of optical communications through soliton solutions in birefringent fibers. *Journal of Optics*. 2024; 1-11.
- [24] Jawad AJM, Abu-AlShaeer MJ. Highly dispersive optical solitons with cubic law and cubic-quintic-septic law nonlinearities by two methods. *Al-Rafidain Journal of Engineering Sciences*. 2023; 1(1): 1-8.
- [25] Jihad N, Abd Almuhsan M. Evaluation of impairment mitigations for optical fiber communications using dispersion compensation techniques. *Rafidain Journal of Engineering Sciences*. 2023; 1(1): 81-92.
- [26] El-Gamel M, Mohamed N, Adel W. Genocchi collocation method for accurate solution of nonlinear fractional differential equations with error analysis. *Mathematical Modelling and Numerical Simulation with Applications*. 2023; 3(4): 351-375.
- [27] Duran S, Durur H, Yavuz M, Yokus A. Discussion of numerical and analytical techniques for the emerging fractional order Murnaghan model in materials science. *Optical and Quantum Electronics*. 2023; 55(6): 571.
- [28] Ozdemir N. M-truncated soliton solutions of the fractional (4+1)-dimensional Fokas equation. *An International Journal of Optimization and Control: Theories & Applications (IJOCTA)*. 2023; 13(1): 123-129.
- [29] Isah MA, Yokus A. Optical solitons of the complex Ginzburg-Landau equation having dual power nonlinear form using φ^6 -model expansion approach. *Mathematical Modelling and Numerical Simulation with Applications*. 2023; 3(3): 188-215.